

This is a repository copy of *Incoherent structural relaxation of fivefold twinned nanowires*.

White Rose Research Online URL for this paper:

<https://eprints.whiterose.ac.uk/id/eprint/60357/>

Version: Submitted Version

Article:

Fu, Xin, Jiang, Jun, Zhang, Wenzheng et al. (1 more author) (2008) Incoherent structural relaxation of fivefold twinned nanowires. *Applied Physics Letters*. 043101. ISSN 0003-6951

<https://doi.org/10.1063/1.2963352>

Reuse

Items deposited in White Rose Research Online are protected by copyright, with all rights reserved unless indicated otherwise. They may be downloaded and/or printed for private study, or other acts as permitted by national copyright laws. The publisher or other rights holders may allow further reproduction and re-use of the full text version. This is indicated by the licence information on the White Rose Research Online record for the item.

Takedown

If you consider content in White Rose Research Online to be in breach of UK law, please notify us by emailing eprints@whiterose.ac.uk including the URL of the record and the reason for the withdrawal request.

Incoherent structural relaxation of fivefold twinned nanowires

Xin Fu,^{1,2} Jun Jiang,^{1,2} Wenzheng Zhang,¹ and Jun Yuan^{2,3,a)}

¹Laboratory of Advanced Materials, Department of Materials Science and Engineering, Tsinghua University, Beijing 100084, People's Republic of China

²Beijing National Center for Electron Microscopy, Tsinghua University, Beijing 100084, People's Republic of China

³Department of Physics, University of York, York YO10 5DD, United Kingdom

(Received 6 April 2008; accepted 16 May 2008; published online 28 July 2008)

Boron carbide nanowires with a fivefold twinned structure have been shown to have regular spaced microtwin lamellas localized in one of the crystalline segments. This defect structure is interpreted as incoherent structural relaxation to relieve the angular excess. A structural model, in terms of a disclination core surrounded by a small angle grain boundary with an intersecting microtwin lamella pair structure, has been proposed and strain analyses suggest it could be a common phenomena for nanowires with large angular mismatch and small twinning formation energy. © 2008 American Institute of Physics. [DOI: 10.1063/1.2963352]

Angular mismatch is a key issue in fivefold twinned nanowires^{1,2} (FTNWs) due to the failure of the regular combination of single crystalline units to satisfy the space filling requirement.^{3,4} The thermodynamic drive for the formation of FTNW is the compensation of the intrinsic elastic energy associated with the angular mismatch by the reduction in surface energy either due to minimization of surface areas or through the exposure of favorable low energy surface facets in materials with large surface energy anisotropy.⁵ The elastic energy however depends strongly on the mode of structural relaxation adopted by FTNWs. In FTNWs with small diameters, elastic energy consideration has lead to either coherent lattice transformation (homogeneous strain)⁵ or a star-disclination distortion (inhomogeneous strain).⁶ Above a critical diameter, we expect that the nanowires either revert back to a single crystalline structure or adopt an incoherently relaxed structure involving extended defects⁴ such as dislocations.⁷ Kinetics is expected to blur but not change this picture much. However, systematic experimental investigation for structural relaxation in FTNW systems is currently lacking.⁸ As many properties of FTNWs depend critically on the defects present,⁹ a through study is vital to the scientific understanding of these materials.

In this paper, we report a detailed experimental study of the structural relaxation in boron carbide (B_4C) nanowires.¹⁰ We show that the internal structure of the nanowires is consistent with a fivefold cyclic twinning and the localized microtwin (MT) lamellas can be interpreted quantitatively as evidence for the negative angular mismatch being relieved by a set of small angle grain boundary (SAGB) in one of the crystalline segments. We also show by internal strain energy analysis that this structural relaxation mode can be energetically favorable, hence a common feature for FTNWs with a large angular mismatch and small twinning energy.

Figure 1 shows the result of a side-view transmission electron microscopy (TEM) of a B_4C nanowire. The electron diffraction pattern in Fig. 1(a) can be successfully interpreted as a composite of diffraction patterns from all five crystallites individually labeled as T1–T5, respectively, where the

twinning systems between them are assumed being $\{100\}_r$, $\langle 011 \rangle_r$ (the subscript r refers to the rhombohedral representation of B_4C unit cells). This is structurally related to the FTNW discovered in boron suboxide.² The dark-field (DF) electron microscopy images using the marked diffracted beams in Fig. 1(a) show a reasonable correspondence between the diffracting regions and the projection from the proposed cross-section of the nanowire [Figs. 1(b)–1(f)], particularly so for T1, T3, and T4. The patched diffraction contrasts for T2 and T5 may be due to their overlap with the strongly diffracting T3 and T4, respectively.

The crystallography analysis suggests that there is a negative angular mismatch of 5° for the unrelaxed B_4C

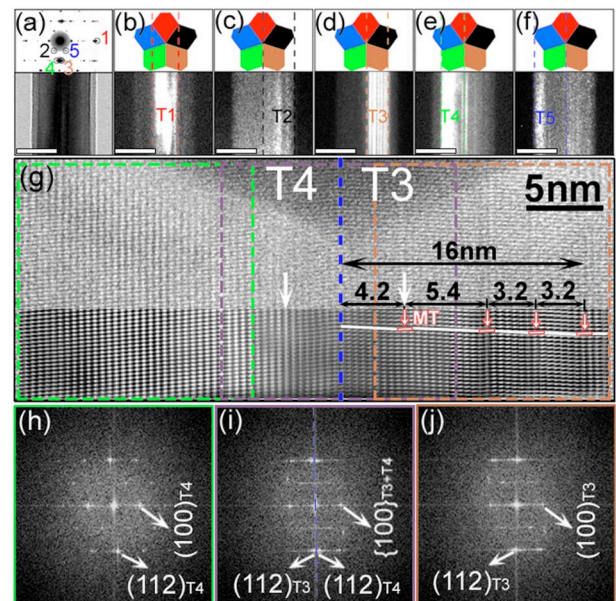


FIG. 1. (Color online) (a) The bright field image and the corresponding diffraction patterns of a B_4C FTNW. (b)–(f) The DF images of five crystallites aligned with the corresponding segments in the cross-sectional model. In (a)–(f), the scale bar is 50 nm. (g) The HR image of the same regions shown in (a). The dashed blue line indicates the interface between T3 and T4. The Fourier filtered images are also displayed in the lower part of (g), the (112) planes of T3 and the MTs are marked by the zigzag solid line. (h)–(j) FFT results from the areas enclosed by colored squares.

^{a)}Electronic mail: jy518@york.ac.uk.

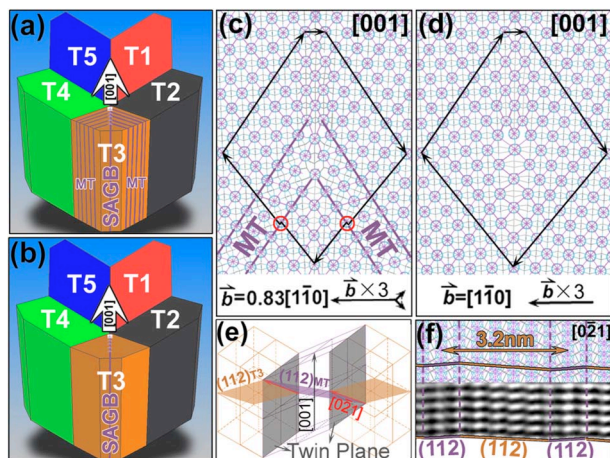


FIG. 2. (Color online) [(a) and (b)] The schematics of the two structural relaxation models of the B_4C FTNW SAGB+MT and SAGB respectively. [(c) and (d)] The cross-sectional view of the atomic structure of the dislocation cores, respectively, together with the effective Burgers circuits and the unbalanced displacements drawn by black arrowed lines. (e) The relationship between the nanowire axis (the $[001]_r$ direction) and the side view observation direction (the $[021]_r$ direction). (f) The direct comparison of HRTEM observation with the projecting atomic structure of the SAGB+MT model.

FTNW.¹⁰ The first evidence suggesting an incoherent structural relaxation mechanism to relieve the resulting stress is the observation of four distinct parallel dark lines along the growth direction in the DF image of T3 [Fig. 1(d)]. To understand their origin, a high-resolution TEM (HRTEM) image [Fig. 1(g)] of the FTNW has been recorded. Because of the overlap of T1, T2 (T5), with T3 (T4), the HRTEM images have information from T1 and T2 (T5) superimposed. To extract the original information specific to T3 and T4, the HRTEM images are Fourier filtered to only include two sets of parallel Fourier spatial frequencies corresponding to the $(100)_r$ and $(112)_r$ spots in the $[021]_r$ zone-axis diffraction pattern and the result is shown in the lower part of Fig. 1(g). The filtered HRTEM image clearly demonstrates that the lattice image of T4 is almost homogeneous outside of a core region delimited by two white arrows, but that of T3 shows lattice distortion such as planar defects corresponding to the dark lines in the DF image of T3. The fast Fourier transform (FFT) of the areas enclosed by colored squares in Fig. 1(g) has also been displayed in Figs. 1(h)–1(j). The blurred $(112)_r$ spots in Fig. 1(j) are different from that in Fig. 1(h), but similar to that in Fig. 1(i), which is taken from the $\{100\}_r$ -type twinning interface between T3 and T4. This result indicates that the planar defects in T3 are $\{100\}_r$ -type MT lamellas. The spacing between the primary twinning interface (between T3 and T4) and the first MT lamella is 4.2 nm, and the spacing between the adjacent MT lamellas is 5.4, 3.2, and 3.2 nm, respectively [Fig. 1(g)].

The experimental result may be understood in terms of a defect structural model proposed in Fig. 2(a). It consists of a star-disclination core and a stress-relieving SAGB in the middle of T3 augmented by a set of intersecting MT lamella pairs (SAGB+MT). The twinning relationship within the MT lamellas is the same as that between the five crystallites of such a nanowire. The SAGB consists of an edge-dislocation array. The existence of MT lamella pairs terminating at each of the dislocation cores is a characteristic fea-

ture of this model. One can show that the existence of MT lamella pairs is favorable energetically by drawing an effective Burgers circuit around an edge dislocation with and without the intersecting MT lamella pairs [Figs. 2(c) and 2(d)]. Without MT lamella pairs, the edge dislocations in the SAGB have Burgers vector of $[1\bar{1}0]_r$. With MTs (each MT lamella has two layers of close packing boron clusters) contributing displacements of $0.83[101]_r$ on the $(010)_r$ plane and $0.83[0\bar{1}\bar{1}]_r$ on the $(100)_r$ plane, the effective Burgers vector of dislocation-MT-pair complex is $0.83[1\bar{1}0]_r$, determined from a sum of $0.83[101]_r$ and $0.83[0\bar{1}\bar{1}]_r$. This is consistent with the Burgers circuit shown in Fig. 2(c), where the total displacements of the kinks induced by the MT lamella are $0.17[\bar{1}0\bar{1}]_r$ and $0.17[011]_r$, respectively. As the dislocation energy scales with the amplitude of the Burgers vector squared but the density of the dislocations only scales inverse linearly with the Burgers vector, the reduction of the effective Burgers vector means a real reduction in the internal elastic energy. The width of the MT lamella as small as two atomic layers is most effective in relieving the atomic lattice compression and dilation near the cores of the edge dislocations [Fig. 2(c)].

Experimental evidence supporting this model is the existence of MT lamella as well as the close match of their theoretical width and spacing with the experimental observation. For this it is helpful to know that crystallographically [Fig. 2(e)] the MT lamella seen in the $[001]_r$ projection [Fig. 2(c)] is the same as MT lamella observed in the experiment along the $[021]_r$ projection. Thus, we see that a width of the MT lamella of equivalently two layers of close packing boron clusters is consistent with the experimental finding [Fig. 1(g)]. The MT lamella spacing is further determined by the dislocation spacing. The mismatch angle of 5° and the effective Burgers vector of $0.83[1\bar{1}0]_r$ give rise to an average dislocation spacing of 5.3 nm along the $[110]_r$ direction corresponding to a MT lamella spacing of 3.2 nm from the side-view observation [Fig. 2(f)]. This is exactly the same as observed; except for the spacing between the inner most pair of MT lamella [Fig. 1(g)]. The latter can also be qualitatively understood as we think that a part of the stress could be relieved by the core of the nanowire which could be coherently relaxed as in a star-disclination model.⁶ Experimentally, this is consistent with the observed contrast difference in the lattice image near the center of the nanowire compared with that of the rest of T4 [Fig. 1(g)]. In our case, the spacing of the first set of MT lamella is then determined by the competition of the relaxation via star-disclination in the core and the SAGB+MT defect complex inside the shell.

The energetics of such a defect model can be compared with other alternatives quantitatively by assuming that the nanowire is an infinitely long cylinder with a constant surface area and surface tension. Figure 3 shows the dependence of internal strain energy (per unit length) as function of nanowire radius. In the pure star-disclination model, the internal strain energy increases exponentially with the radius of the nanowire.^{6,11} According to the SAGB model [Fig. 2(b)], the internal strain energy is dominated by the elastic energy of the dislocation array. This can be estimated¹² and is found to increase linearly with the radius of the nanowire (the SAGB1 curve in Fig. 3). To estimate the strain energy for the

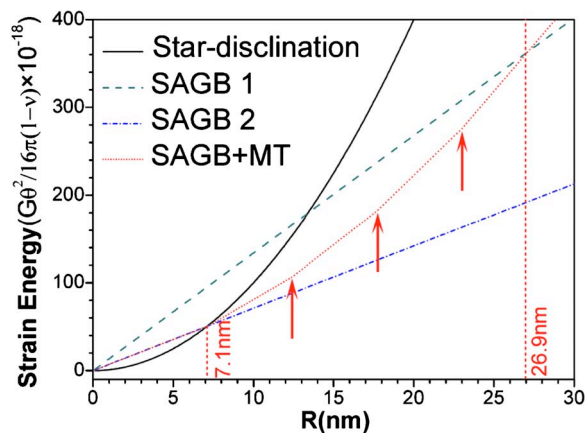


FIG. 3. (Color online) The internal strain energies as a function of the nanowire radius for the star-disclination model, the pure SAGB model (SAGB1) and the SAGB+MT model respectively (SAGB2 did not include the additional twin boundary energy). The arrows indicate the expected positions of the dislocation.

SAGB+MT model [Fig. 2(a)], we have modified the simple SAGB theory¹² by treating the strain energy of the dislocation-MT-pair complex in terms of two contributions: one is the strain energy of the dislocation array with an equivalent Burgers vector of $0.83[1\bar{1}0]$, and the other is the twin boundary energy. Thus, the former is again a linear relationship with the nanowire radius, but with a reduced slope because of the smaller effective Burger vector (the SAGB2 curve in Fig. 3). The inclusion of the additional twin boundary energy results in an upward bend of the strain energy curve (the SAGB+MT curve in Fig. 3), which eventually crosses with the upper linear relationship for the defect model involving SAGB only. This implies that the proposed SAGB+MT defect systems can potentially be stable over a finite range of nanowire radius and is particularly favorable in material systems with a small energy for the twinning surfaces. To check out this, we may assume that the crossover into the pure SAGB defect system happens at the radius of the currently examined nanowire [26.9 nm corresponding to about 16 nm in the viewing plane of Fig. 1(g)]. This gives an upper limit to the $\{100\}_r$ twin boundary energy (per unit area) being only 25% of that of SAGB. We can also use the disclination theory^{6,11} to calculate the crossover from pure star-disclination to SAGB+MT complex. If we define the distance of the first dislocation to the center of the nanowire as the crossover from star-disclination type relaxation model to the SAGB+MT complex, we find that an assumption of dislocation core radius of 1.7 nm is then sufficient to produce an experimentally inspired critical radius of 7.1 nm [or 4.2 nm when viewed in the $[0\bar{2}1]_r$ orientation in Fig. 1(g)].

The dislocation core radius used is a reasonable value for the validity of the dislocation model used and is also consistent with the atomic structure of boron carbide.¹³

It is clear that the proposed structural model is energetically more favorable for multiply twinned nanowires with a large radius and a large angular mismatch. This is consistent with the lack of such MT defects in boron suboxide multiply twinned nanowires with an even larger radius of 40 nm,² another superhard materials but with almost zero angular mismatch. Due to the similar close-packing structure our result should also be relevant to fcc-based multiply twinned nanowire systems. For example, our model is consistent with the defect structure observed in multiply twinned nanoparticles of silicon¹⁴ and germanium³ where the role of MTs is taken up by stacking faults, even though the relaxation is more complicated because of the complex interaction of defect with the surface.¹⁵

Traditionally, the exceptional property of nanowires and nanowiskers are thought to be the absence of lattice defects common in their bulk counterpart.¹⁶ Our result clear shows that this is not valid for nanowires with intrinsic growth defects such as discussed here. We hope that our detailed relaxation model provide a realistic starting point to take these defects into account in understanding of the physical properties of incoherently relaxed nanowire structure.

This research is supported by The National Basic Research Program (Grant No. 2002CB613500) from Chinese Ministry of Science and Technology.

¹A. J. Melmed and R. Gomer, *J. Chem. Phys.* **34**, 1802 (1961); I. Lisiecki, A. Filankembo, H. Sack-Kongehl, K. Weiss, M. P. Pileni, and J. Urban, *Phys. Rev. B* **61**, 4968 (2000).

²J. Jiang, M. H. Cao, Y. K. Sun, P. W. Wu, and J. Yuan, *Appl. Phys. Lett.* **88**, 163107 (2006).

³H. Hofmeister, *Cryst. Res. Technol.* **33**, 3 (1998).

⁴V. G. Gryaznov, J. Heydenreich, A. M. Kaprelov, S. A. Nepijko, A. E. Romanov, and J. Urban, *Cryst. Res. Technol.* **34**, 1091 (1999).

⁵S. Ino, *J. Phys. Soc. Jpn.* **27**, 941 (1969).

⁶R. de Wit, *J. Phys. C* **5**, 529 (1972).

⁷L. D. Marks, *Rep. Prog. Phys.* **57**, 603 (1994); Y. T. Pei and J. Th. M. De Hosson, *Acta Mater.* **49**, 561 (2001).

⁸H. Y. Chen, Y. Gao, H. R. Zhang, L. B. Liu, H. C. Yu, H. F. Tian, S. S. Xie, and J. Q. Li, *J. Phys. Chem. B* **108**, 12038 (2004).

⁹H. Hakkinen, M. Moseler, O. Kostko, N. Morgner, M. A. Hoffmann, and B. von Issendorff, *Phys. Rev. Lett.* **93**, 093401 (2004); B. Wu, A. Heidelberg, J. J. Boland, J. E. Sader, X. M. Sun, and Y. D. Li, *Nano Lett.* **6**, 468 (2006).

¹⁰X. Fu, J. Jiang, C. Liu, and J. Yuan (unpublished).

¹¹Wen Huang and T. Mura, *J. Appl. Phys.* **41**, 5175 (1970).

¹²W. T. Read and W. Shockley, *Phys. Rev.* **78**, 275 (1950).

¹³F. Mauri, N. Vast, and C. J. Pickard, *Phys. Rev. Lett.* **87**, 085506 (2001).

¹⁴S. Iijima, *Jpn. J. Appl. Phys., Part 1* **26**, 365 (1987).

¹⁵A. Howie and L. D. Marks, *Philos. Mag. A* **49**, 95 (1984).

¹⁶A. J. Cao and Y. G. Wei, *Phys. Rev. B* **74**, 214108 (2006).